ÉCOLE POLYTECHNIQUE
FÉDÉRALE DE LAUSANNE

Research plan.

Understanding the dissociation dynamics of UV excited peptides.

Presented by
Aleksandra
Zabuga

Under The Supervision of
Professor Thomas R. Rizzo

Laboratoire de Chimie Physique Moléculaire

2011

Table of Contents.

TABLE OF CONTENTS. 2

1 INTRODUCTION. 3

2 IRLAPS. 4

3 THEORETICAL MODELS. 7

3.1 MODEL BASED ON THE ELECTRONIC ABSORPTION OF A SINGLE AROMATIC AMINO ACID. 7
3.2 ELECTRON DRIVEN PROTON TRANSFER (EDPT) MODEL. 9
3.3 INITIAL LOSS OF THE SIDE CHAIN. 11

4 EXPERIMENTAL APPROACH TO TEST THEORETICAL MODELS. 12

4.1 PROPOSED SCHEME. 12
4.2 EXPERIMENTAL SETUP. 14

5 FIRST EXPERIMENTAL RESULTS. 15

6 REFERENCES. 16

1 Introduction.

The biological functions of proteins in the living organisms are largely determined by their three-dimensional structures, which adapt to the changing biological environments.

Spectroscopic investigations of isolated peptides in the gas phase in the absence of solvent molecules are of high importance. They provide information about pure intramolecular interactions that is crucial for modeling molecular behavior in vivo.

The difficulty in studying molecules of biological interest in the gas phase arises from their low vapor pressure and thermal instability. First experiments on neutral isolated amino acids used the combination of vaporization by heating and supersonic expansions [1-4]. The rapid cooling achieved in a supersonic expansion greatly simplifies the spectra such that different stable conformers could be identified [3]. Similar approaches have been applied to study a variety of biological molecules ranging from individual amino acids [5] to small peptides [6-10]. Different spectroscopic techniques were applied such as IR-UV, UV-UV and IR-IR-UV [11] multiple-resonance spectroscopy.

With the invention of soft ionization techniques such as electrospray ionization (ESI) [12], large biomolecules and even noncovalentely bound complexes could be transferred into the gas phase without thermal decomposition [13]. The fact that in an ESI source biomolecules are ionized is not unfavorable, because biological molecules in solution often carry a charge, which can have a large effect on their photophysics [14, 15]. Weinkauf and co-workers coupled an ESI source with a liquid nitrogen cooled Paul trap to record a spectrum of protonated tryptophan [16]. Its spectrum was broad, in contrast to the neutral tryptophan, which exhibits well-resolved spectral features at low temperature [3]. In our group, a cold 22-pole ion trap based on the design of Gerlich [17] was built and coupled to a home-made tandem mass spectrometer, which enables more efficient cooling compared to the Paul trap [18]. However, the spectra of protonated tryptophan still were broad, which was later attributed to the electronic properties of tryptophan. In contrast, the electronic spectrum of protonated tyrosine shows sharp, well-resolved features (**Figure 1**).

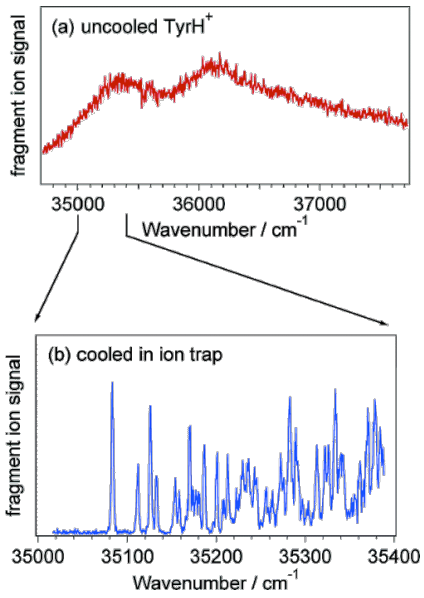

Figure 1. Electronic photofragmentation spectra of (a) uncooled TyrH+;
(b) TyrH+ that has been cooled in the 22-pole ion trap[18].

As one considers larger biological molecules, the large number of stable conformers and the high density of vibrational levels would be the major factors of spectral congestion. Whereas the problems of spectral complexity could be overcome by increasing IR laser resolution or by preselecting single conformers prior to performing spectroscopic interrogation (e.g. by combining with ion mobility), the lower dissociation yield limits the ability to obtain the spectra. The method used in our laboratory to obtain the IR spectra of biomolecular ions is based on the UV photofragmention, when the signal is recorded by means of detecting the products of dissociation under the UV laser excitation. If the molecules dissociate directly from an excited electronic state the process is fast and the dissociation rate should not scale with the molecular size. However, if the dissociation occurs after internal conversion followed by intramolecular vibrational redistribution (IVR) on the ground potential enegy surface, the fraction of molecules that dissociate after the UV excitation would strongly scale with their size. In the larger molecules there are more vibrational modes where the energy can be stored and one would need to add energy into the system to promote the dissociation.

In order to increase the dissociation yield, it was suggested to assist the photofragmentation by a CO_2 laser, the scheme that Settle and Rizzo first implemented to detect weak overtone transitions of the small neutral molecules [19] and that was called in the following papers infrared laser-assisted photofragment spectroscopy (IRLAPS) [20]. This approach is similar to the work of Lee and co-workers, who had used infrared multiphoton dissociation (IRMPD) to selectively detect vibrational excitation of hydrated hydronium cluster ions [21]. The IRLAPS technique was adapted in our laboratory for measuring the electronic and vibrational spectra of large biomolecular ions with sizes of up to 76 amino-acids (ubiquitin) [22] and in all the cases the CO_2 laser selectively enhances a particular dissociation channel that seems not to be the one of lowest energy. In order to predict the efficiency of the IRLAPS method for the application to even larger molecules, one needs to understand the dissociation mechanism, and this is the primary subject of present thesis proposal.

2 IRLAPS.

In Figure 2 it is shown how the IRLAPS method is experimentally applied to measure the electronic and vibrational spectra of large peptide ions [23]. In the case of the UV-only induced photofragmentation, the fraction of molecules that dissociate decreases as the number of vibrational modes increase. The mechanism is not completely understood, but one can consider the formation of the radical species after the UV excitation that would require the absorption of additional energy for the subsequent dissociation. This energy could be introduced into the system by using a CO_2 laser pulse that would promote the fragmentation of the radicals by infrared multiphoton excitation (IRMPE).

If the dissociation occurs first by internal conversion to the ground electronic state followed by IVR and unimolecular dissociation, the rate would also strongly scale with the number of vibrational modes and get slower as the size of the molecules increases. The additional use of a CO_2 laser promptly after the UV laser pulse would consequently increase the dissociation rate by increasing the vibrational energy of the pre-excited molecules.

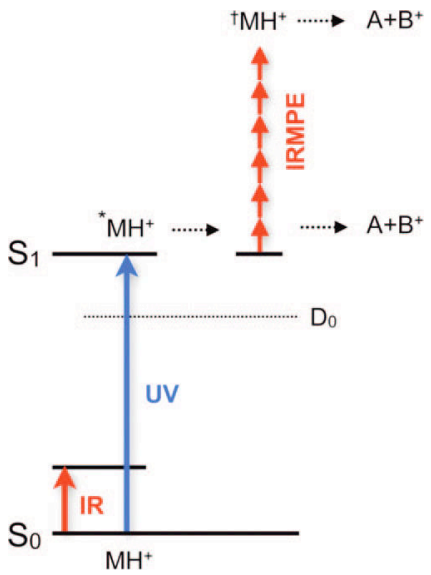

Figure 2. The scheme of the IRLAPS method.

The electronic (**Figure 3**) and vibrational (**Figure 4**) spectra of the protonated peptides show the same spectroscopic features with or without the assistance of the CO_2 laser. This indicates that IRLAPS is a powerful technique to increase the signal to noise ratio (S/N) without other impact on the IR-UV spectroscopic response.

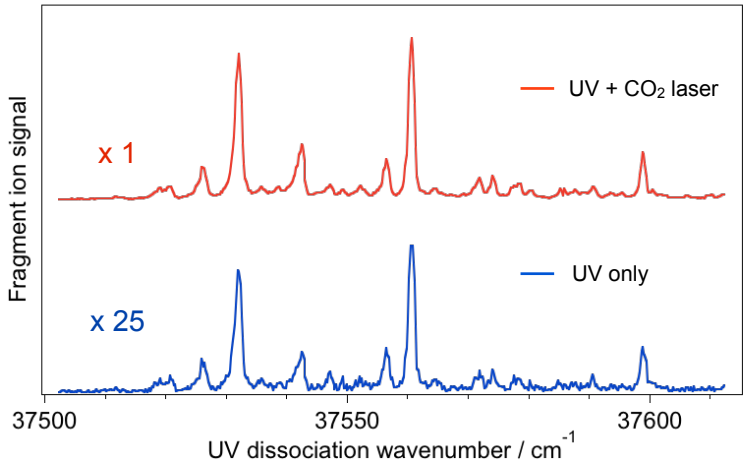

Figure 3. Electronic spectra of Ac-Phe-$(Ala)_5$-Lys-H^+ obtained by UV fragmentation (blue lines, scaled 25 times) and by UV excitation assisted by IRMPE (red lines). The monitored fragment corresponds to the loss of phenylalanine side chain. Adopted from [24].

When IRLAPS was first implemented to accelerate the dissociation of the charged peptides it was expected that the CO_2 laser would act on statistical dissociation channels after the UV pre-excitation followed by internal conversion. However, it turned out that the preferred dissociation channel in all investigated peptides was the aromatic side chain loss. The fragment signal that corresponds to C_α-C_β bond cleavage is increased by approximately two orders of magnitude in the case of phenylalanine (Phe) chromophores and by approximately one order of magnitude for tyrosine (Tyr) and tryptophan (Trp) [24]. The other fragmentation channels that correspond to backbone cleavages and that are the major channels of fragmentation in IRMPD experiments from the ground electronic state (or collision induced dissociation) are not strongly enhanced.

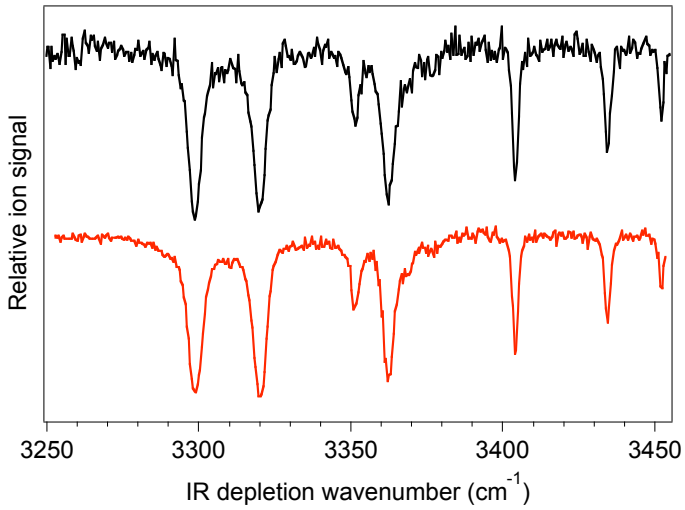

Figure 4. IR-UV depletion spectra of Ac-Phe-$(Ala)_5$-Lys-H^+, obtained by fixing UV laser wavenumber at 37560 cm^{-1} without and with the assistance of IRMPE (black and red trace respectively). Adopted from [24].

It is surprising that independent of the probe chromophore, the cleavage of the C_α-C_β bond is the preferred dissociation channel, even though this is not the weakest bond in the ground electronic state, which can be seen from IRMPD-assisted dissociation of the parent molecules (Figure 5).

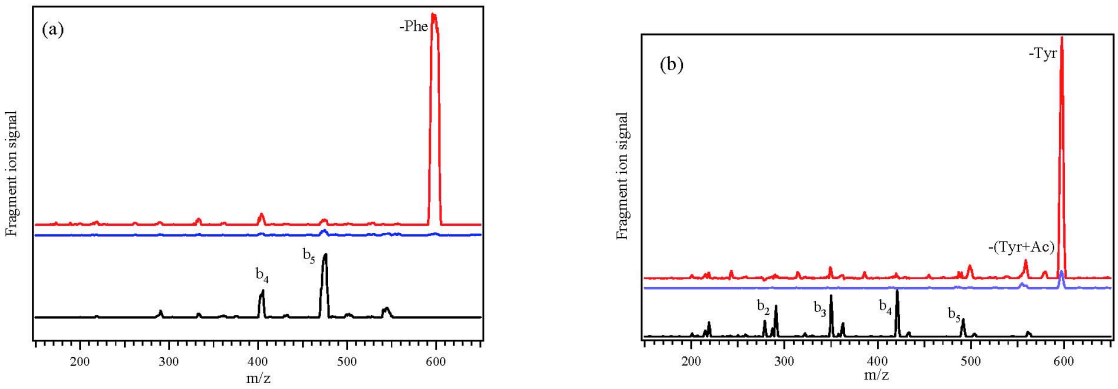

Figure 5. Photofragment mass spectra of (a) Ac-Phe-$(Ala)_5$-LysH^+ and (b) Ac-Tyr-$(Ala)_5$-LysH^+ obtained by UV photofragmentation (blue trace) and by UV-CO_2 laser excitation (red trace). The black traces correspond to the CO_2 laser only photofragment spectra (IRMPD-assisted dissociation) [24].

The increase of the fragmentation due to the side chain loss was investigated as a function of the delay between the UV and the CO_2 lasers. It appeared that the enhancement occurs when the delay between UV and CO_2 lasers is less than 100 ns (Figure 6) that reflects the rise time of the CO_2 laser. Then the signal decreases and reaches an asymptotic value at 1 ms that is still higher than the UV only induced fragmentation [24]. The initial oscillations and decay of the signal correspond to the motion of the ions in the 22-pole ion trap. This means that the fraction of UV pre-excited molecules, which dissociate under the CO_2 laser pulse, is almost constant within the investigated delay range between the UV and the CO_2 lasers. The fact that non-statistical fragment was observed at long times after UV excitation suggest that the dissociation may occur directly from the excited electronic state or from a new intermediate species, which is formed promptly after UV excitation and lives for several milliseconds.

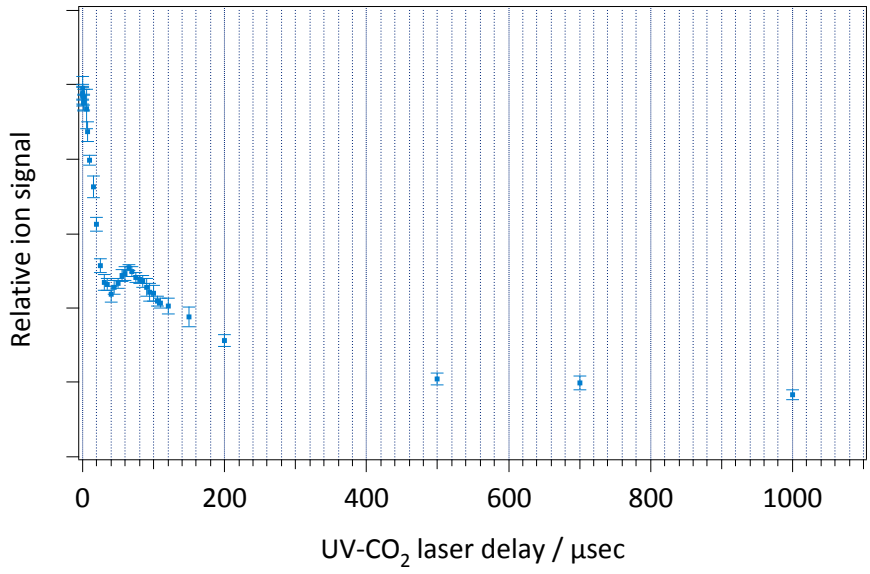

Figure 6. Relative ion signal corresponding to the side chain loss fragment of Ac-Phe-$(Ala)_5$-$LysH^+$ as a function of the time delay between the UV and the CO_2 lasers. Adopted from [24].

In order to understand the fragmentation process, the mechanism of the formation of the intermediate and its structure need to be studied in detail. Theoretical models that provide possible explanations of the dissociation mechanism will be presented in the following section.

3 Theoretical models.

In order to evaluate whether the IRLAPS technique can be a universal tool to enhance the dissociation of electronically excited biomolecules of increasing size and to predict its efficiency one needs to understand the dissociation mechanism. The possible ways leading to the C_α-C_β bond cleavage in charged peptides are discussed in several models proposed by Jouvet and coworkers and by Sobolewski and Domcke.

3.1 Model based on the electronic absorption of a single aromatic amino acid.

The mechanism of photoinduced C_α-C_β bond cleavage in a single protonated aromatic amino acid was extensively studied in the group of Jouvet and co-workers [25, 26]. The experiments with protonated tryptophan, in which ionic and neutral photofragments are detected simultaneously, revealed two pathways for the C_α-C_β bond rupture, a slow one on a microsecond time scale and a fast one on a nanosecond time scale [25]. On the left side of Figure 7 the slow process, which consists of two steps, is illustrated. First, the UV laser promotes light-induced electron transfer from the aromatic ring to the ammonium group that leads to fast hydrogen loss. In the second step, the newly formed radical cation slowly dissociates by breakage of the C_α-C_β bond. Ab initio calculations [27, 28] attribute the H-loss channel to a direct coupling between the locally excited $\pi\pi^*$ state with a repulsive low lying $\pi\sigma^*$ state that dissociates along the NH bond of the amino group. This fragmentation channel is less accessible in the case of protonated tyrosine because its dissociative $\pi\sigma^*$ configuration is higher in energy. In contrast to tryptophan the H-loss channel was not observed for tyrosine, suggesting the presence of a different dissociation mechanism.

The second dissociation pathway, presented on the right side of Figure 7, involves electron transfer from the aromatic ring to the oxygen of the carboxy group upon UV laser excitation with subsequent fast proton transfer from the NH_3^+ group toward the C=O of the carboxy group. This results in the formation of biradical cation, that dissociates *via* C_α-C_β bond cleavage within 100 ns [26]. The comparative study of the fragmentation of protonated tyramine and tryptamine, (which correspond to decarboxylated tyrosine and tryptophan, respectively), showed slower fragmentation in the case of tryptamine and no fragmentation *via* C_α-C_β bond cleavage in the case of tyramine. This suggests that the presence of the carboxylic group is crucial for the fast fragmentation.

In IRLAPS experiments with protonated Phe previously done in our group, fast C_α-C_β bond rupture was observed (<100 ns after UV excitation) [24]. Experiments with protonated phenethylamine (i.e., decarboxylated Phe) revealed no cleavage of the C_α-C_β bond. This confirmed the role of the COOH group in the dissociation mechanism after UV excitation, but according to the fast dissociation pathway model [26] electron transfer to the COOH group leads to the formation of a short living biradical cation. In the larger peptides investigated with the IRLAPS technique after UV laser excitation, the intermediate lives at least few hundreds of μs (Figure 6).

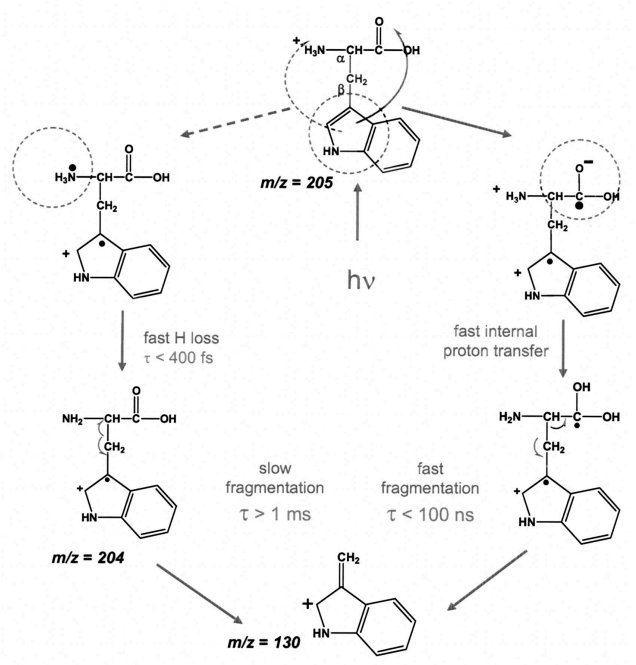

Figure 7. Scheme of the two mechanisms for C_α-C_β bond cleavage in tryptophan. Right side: the excited state mechanism, through proton transfer toward the carboxy group. Left side: The two-step mechanism. Slow dissociation of the radical cation subsequent to the H loss.

Furthermore, according to the fast mechanism proposed by Lucas et al. [26], preventing proton transfer from NH_3^+ group after electronic excitation should inhibit fragmentation *via* the C_α-C_β bond cleavage. In an IRLAPS experiment, the peptide Ac-Phe-$(Ala)_5$-$LysH^+$ was substituted with 18-crown-6-ether in order to block the charge [24]. It turned out that under UV only excitation without the CO_2 laser assistance there were no fragments corresponding to the C_α-C_β bond cleavage, whereas after UV-CO_2 laser excitation this fragmentation channel was observed, in

contrast to the expectation. This means that the charge doesn't play an active role in the formation of an intermediate state from which the CO_2 laser promotes dissociation.

The model might explain the dissociation of protonated phenylalanine and other single aromatic amino acids. However, for the larger peptides charge seems not to be actively involved in the dissociation mechanism and the model doesn't explain the fact that C_α-C_β bond cleavage occurs at long times after electronic excitation.

3.2 Electron driven proton transfer (EDPT) model.

The electron-driven-proton transfer model was derived from the studies of the excited states of hydrogen bonded systems by Sobolewski and co-workers [29]. In proteins in the ground electronic state, hydrogen bonds are formed between CO and NH groups of the backbone, and this plays an essential role on their three-dimensional structure and photophysics. Excited electronic states of polyatomic molecules have open shell configurations and require the exploration of high-dimensional potential energy surfaces over wide regions, which renders their calculations challenging. Recently, the electron driven proton transfer deactivation mechanism after UV excitation was established for the one of the low energy conformers of Gly-Phe-Ala peptide by *ab initio* calculations [30].

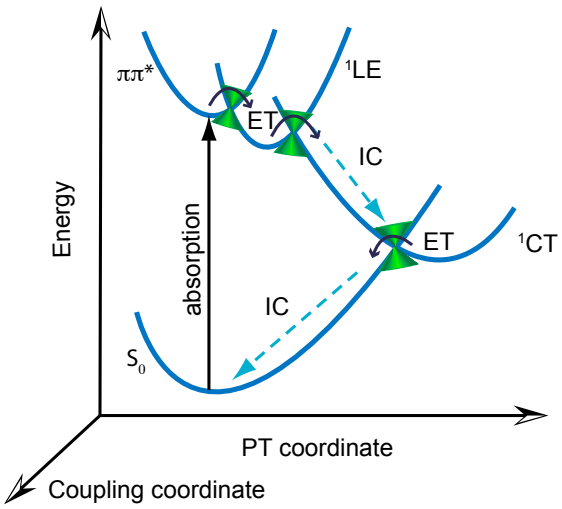

Figure 8. Schematic representation of the EDPT process in intramolecularly hydrogen-bonded systems. Abbreviations: LE, locally excited state; CT, charge transfer state; ET, electron transfer; IC, internal conversion.

According to this model in the first step the UV laser transfers the population from the ground electronic state of the peptide to the lowest electronically excited ππ* state of the phenyl ring. One of the locally excited states (^{1}LE), lies slightly lower in energy than the ππ* state, which causes radiationless relaxation from the ππ* state to the ^{1}LE state through a conical intersection. There exists also an optically dark charge transfer state (CT) that has a conical intersection with both the ^{1}LE state and the ground electronic state S_0 at its minimum geometry. Population of the CT state involves transfer of the electron from the hydrogen-bonded NH group to the CO group along the intramolecular hydrogen bond. The high polarity of the CT state provides the driving force for the proton transfer following the electron. Afterwards, the electron is transferred back through the CT-S_0 conical intersection and the proton follows, closing the photophysical cycle. The large energy gradients and small mass of the proton ensure the rate of this processes is fast. The electronic energy is converted by the passage through three conical intersections into vibrational energy of the ground state on the timescale of a few fs [29]. This EDPT mechanism is schematically presented in a potential energy diagram on Figure 8.

In the Dugourd group [31] the dynamics of a neutral tryptophan radical formed from a doubly-deprotonated five amino acid peptide *via* electron detachment was studied. The pump-probe experiments revealed that under UV excitation the Trp radical is promptly formed in less than 100 ns due to the loss of the electron and is stable for several milliseconds, so that it can be isolated and irradiated with a visible laser. The visible photofragmentation spectrum of the radical Trp ions shows good agreement with the calculated absorption spectrum that indicates that the rest of the peptide has a weak influence on the optical properties of the radical [31].

If the photoexcitation mechanism in the protonated aromatic peptides is similar to the mechanism in deprotonated peptides, the observation of the chromophore radical by means of visible spectroscopy should be possible in these cases, too. Use of a visible laser instead of a CO_2 laser led to the same fragmentation pattern as in the IRLAPS experiments, where an enhancement of the signal due to C_α-C_β bond rupture was observed. Guidi succeeded to record the visible spectrum of UV pre-excited Ac-Phe-$(Ala)_5$-$LysH^+$ peptide with a Phe chromophore, by a UV-VIS double-resonance technique similar to the scheme in Figure 2 [24]. These results support the assumption that the UV laser induces the formation of a biradical as an intermediate, in which the C_α-C_β bond is the weakest bond. But according to the model of Sobolewski and Domcke for the UV excited-state deactivation of the Gly-Phe-Ala peptide, the biradical formed should be short lived. This contradicts the observations made for larger protonated peptides in our group (Figure 6) as well as in the deprotonation experiments in the group of Dugourd [31]. A possible reason for this could be the existence of another potential minimum in the CT state (Figure 8) corresponding to the stable biradical that could live for several milliseconds and in which the C_α-C_β bond is the weakest.

Sobolewski performed *ab initio* calculations on the Ac-Phe-$(Ala)_2$ –NMe peptide [32] to see if the stable biradical can be formed in larger peptides than Gly-Phe-Ala . Because the model involves EDPT along the hydrogen bond between the CO of the acetylated group of Phe and the NH group of the first ^{1}Ala in the sequence it can be extended for larger peptides with further aminoacids on the C-terminal side.

Figure 9 represents the results of the calculations performed by Sobolewski. In this model the absorption of a UV photon populates the ππ* state of the phenyl ring that relaxes to the low-lying ^{1}LE state as in the case of Gly-Phe-Ala peptide [30]. In addition, there is a low-lying charge transfer state (CT) that has a conical intersection with the ^{1}LE state and that is populated *via* electron transfer to the CO group of the acetylated part of Phe from the NH group of the ^{1}Ala along the intramolecular hydrogen bond. The transfer of the electron induces the proton transfer to the CO group of the acetylated part of Phe, resulting in a COH---N hydrogen bond in a closed biradical. Such a closed biradical should be a short-lived species because it can easily relax to the ground electronic state through a conical intersection including the back-reaction of a proton transfer on a fs timescale. However, after electron driven proton transfer (EDPT) the acetyl group also has enough energy to rotate and then stabilize *via* intramolecular vibrational redistribution (IVR) without the formation of a COH---N hydrogen bond. The resulting product is an open biradical and can live for a long time because the direct access to the conical intersection with the ground electronic state is prohibited. The weakest bond of the open biradical is the C_α-C_β bond. The additional absorption of energy from the CO_2 laser or the visible laser would break the C_α-C_β bond thus promoting fragmentation through this dissociation channel.

This model can describe the dissociation mechanism for the class of peptides in which the internal rotation is hindered by a single hydrogen bond. Breakage of the hydrogen bond due to

the EDPT mechanism would leave the acetyl group free to rotate, which would lead to the dissipation of the energy and prevent the formation of the short-lived, closed biradical. However, the IRLAPS method was also successfully implemented to increase the dissociation yield of protonated peptides with multiple hydrogen bonds where it is hard to identify the moiety free to rotate after EDPT. These molecules are bradykinin, which forms a salt-bridge in a gas phase [33], and cyclic gramicidin S, that forms ß-sheets in solution [34]. In this case one can argue that after EDPT along one of the multiple hydrogen bonds, the released energy is rapidly transferred to the vibrations (*via* IVR) or is used for conformational isomerization so that the broken hydrogen bond cannot be reformed. Whereas in the protected peptides the conformational change can be identified by the rotation of the protecting group, calculations of the biradical need to be performed for each molecule in order to identify the relevant conformations in the case of non-protected peptides.

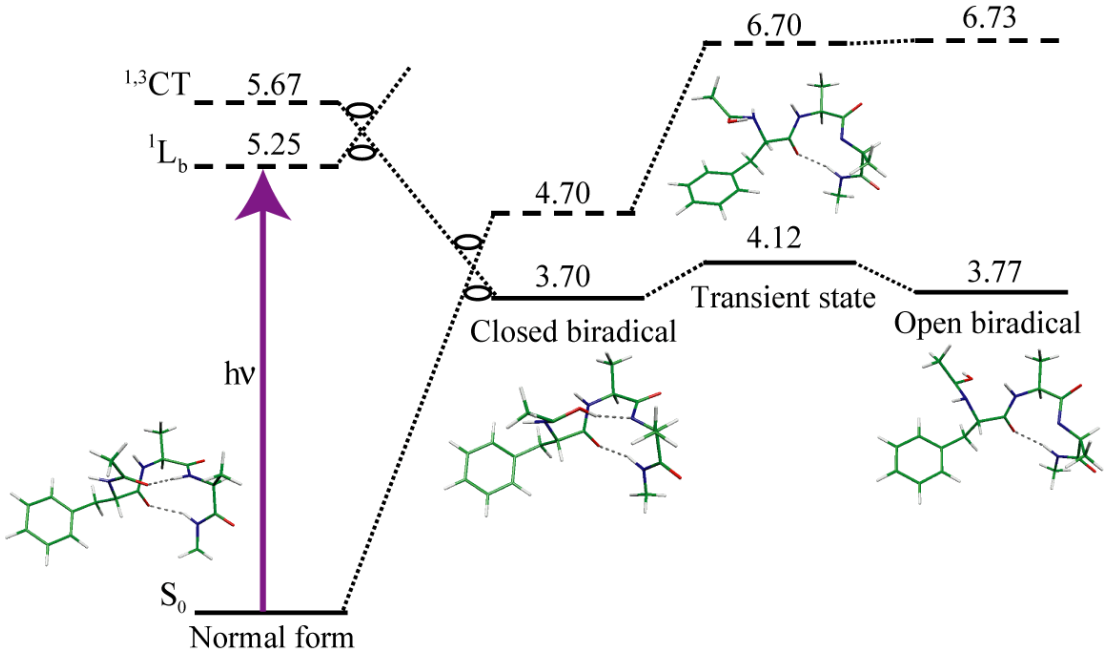

Figure 9. Photophysical scheme of the Ac-Phe-$(Ala)_2$–NMe peptide determined by excited-state ab initio calculations. Numbers denote energy in eV related to the ground state. Solid lines denote states in optimized geometry. Dashed lines denote vertical energy levels calculated at a given geometry. Dotted lines show the adiabatic correlations between the states [32].

3.3 Initial loss of the side chain.

As has been discussed before, the model proposed by Sobolewski, might well describe the experiment, but it lacks the predictive power, because the open biradical structure has to be thoroughly calculated for all non-protected peptides.

The model, proposed by Jouvet [35], involves the initial breakage of the C_α-C_β bond after the UV excitation by the fast mechanism presented on the right side of Figure 7 or a similar one so that the bond cleavage occurs within 100 ns. According to the experimental results, the intermediate forms promptly after the UV excitation and has a lifetime on the order of ms (Figure 6). This could happen if most of the aromatic side chain radical fragments do not leave the parent molecule but stick to the charged backbone fragment of the peptide just after the formation because of a strong cation-π interaction. The aromatic side chain residues from Phe, Tyr and Trp (benzene, phenol and indole respectively), have a quadrupole moment that can interact with the charge of the protonated peptides. The ion-quadroupole interactions decrease with increasing distance proportionally to $1/r^3$ [36], but Dougherty et al. showed a $1/r^n$

dependence with n<2 for aromatic compounds [37]. Aromatic rings possess high electron density in the center of the ring [38], that can provide a potential binding site for cations and that under favorable conditions can even compete with an aqueous environment [37]. The more negative the maximum in electrostatic potential over the center of the aromatic, the stronger the cation-π interaction [39]. A review by Ma and Dougherty presents an overview of cation-π interactions for a wide range of different molecules [39]. Some typical examples for cation-π interaction energies are [40]:

- NH_4^+ - benzene (C_6H_6): 19 kcal/mol,
- NH_4^+ - phenol (C_6H_5OH): 20.5 kcal/mol,
- NH_4^+ - indole: 25.9 kcal/mol.

NH_4^+ can be regarded as a representative for lysine or arginine protonated side chains [41]. These energies can be compared to the critical energy for dissociation of crown ether/NH_4^+ complexes, which ranges from 32 kcal/mol for 12-crown-4 to 41 kcal/mol for 18-crown-6 [42].

Irradiation with a CO_2 laser can easily lead to a breakage of the intermolecular bond between the aromatic side chain and the charged backbone fragment by multiphoton absorption and thus enhance the side chain loss fragmentation signal.

4 Experimental approach to test theoretical models.

4.1 Proposed scheme.

In order to evaluate the proposed models for the IRLAPS mechanism, acquiring a spectrum of the intermediate after UV excitation would be desirable. An IR spectrum of the intermediate state can serve as a benchmark for the calculations, which could in turn help to identify its structure and confirm one of the models. It was shown, by changing the delays between the UV and the CO_2 laser, that UV excitation promotes the parent molecules to an intermediate state with a lifetime of a least a millisecond (Figure 6). In a cold 22-pole ion trap filled with He gas, one millisecond is sufficient to partially cool back down the UV pre-excited molecules. Thus by shining the UV laser right after the arrival of the molecules into the 22-pole ion trap and by letting them cool down during approximately 1 ms, one could measure highly resolved spectra of the cold intermediate.

Because the species that are formed are likely radicals, they should absorb visible light and fragment upon the absorption. Indeed, Guidi used a visible laser instead of the CO_2 laser after UV excitation and detected the chromophore side chain loss as the main dissociation product [24]. Then she recorded an electronic spectrum of the intermediate cation in the region 17000 - 20500 cm^{-1} with a delay of 200 ns between the UV and the visible laser. These experiments were carried out using a peptide with a phenilalanine (Phe) chromophore. Loss of the side chain from the Phe results in the formation of a benzyl radical. Heaven et al. recorded a highly resolved electronic spectrum of the benzyl radical in a supersonic free jet expansion [43]. The intense vibronic progression appears further shifted to the blue in the range 22275 - 22475 cm^{-1}. If the visible spectrum of the cooled UV pre-excited molecules containing Phe as a chromophore will show comparable spectra, this will support the model in which the aromatic side chain sticks to the charged rest of the molecule. Joly et al. obtained the visible spectrum of the UV-excited doubly deprotonated Trp-$(Val)_4$ peptide and affirm the formation of an indolyl radical after electron detachment [31]. The experimental spectrum was in a good agreement with the calculated spectrum of the neutral indolyl radical. Because of the low resolution of the experimental spectra, a confirmation by high-resolution spectroscopy would be desirable.

Maybe more promising but probably also more challenging would be an IR spectroscopic experiment of the intermediate species after cooling them for approximately 1 ms. Initially, using only the UV laser, a small portion of the parent molecules in the 22-pole ion trap will be excited. IR-UV photofragment spectroscopy cannot be done on the intermediate species because of the photofragmentation of the parent molecules. To eliminate the background signal IR-VIS spectroscopy can be applied, because the parent molecules do not absorb visible light. Highly resolved IR spectra along with the calculations can help to establish the structure of the UV excited molecules and the dissociation dynamics.

According to the theoretical model described in chapter 3.3, the interaction between the charged backbone and the side chain fragment after UV pre-excitation should be weaker than a typical covalent bond, but too strong to be broken by low energy collisions. One can also try to test if one IR photon is sufficient to break the bond between the benzyl radical and the charged rest of the molecule. Assuming the cation-π interaction of approximately 19 kcal/mol, breakage of the intermolecular interaction in one photon process would require the energy of a photon around 6600 cm^{-1}.

$$19kcal/mol = \frac{19 \cdot 4.2 \cdot 10^{3}\, J/mol}{6.022 \cdot 10^{23}\, 1/mol} \approx 13.25 \cdot 10^{-20} J$$

$$E = \frac{h \cdot c}{\lambda} \Rightarrow \lambda^{-1} = \frac{h \cdot c}{E} = \frac{6.62 \cdot 10^{-34}\, m^2 kg/s \cdot 3 \cdot 10^{8}\, m/s}{13.25 \cdot 10^{-20} J} \approx 6600 cm^{-1}$$

$$\lambda \approx 1.5 \mu m$$

CH stretching vibrations appear in the spectral region 2600 - 3000 cm^{-1}, whereas OH stretching vibrations are more energetic 3400 - 3700 cm^{-1}. Thus in order to break the cation-π interaction one would probably need at least three photons or to excite an OH stretch overtone. The Phe side chain contains only C and H atoms and coupling with the other OH vibrations is most likely not efficient. In the case of Tyr two photons for excitation its OH stretching vibration should be sufficient. Consequently, for first attempts to record an IR spectrum of the cold intermediate Tyr was chosen as a chromophore.

Typical pulse energies of the optical parametric oscillator (OPO) IR source are around 8 mJ. Focusing of the beam will probably promote multiphoton absorption and make it possible to record the vibrational spectrum using only one IR laser. If the energy is not sufficient to produce photofragments, an IR-VIS double-resonance spectroscopic scheme will be used.

One main experimental difficulty is to produce enough UV pre-excited molecules in the sample volume probed by the spectroscopic lasers after cooling. Svendsen et al. simulated the motion of the ions inside the 22-pole trap and Guidi observed the effect experimentally [24]. After 200 µs delay between the two lasers (IR and UV or UV and CO_2) the detected photofragment signal drops by a factor of two, because the irradiated ions move out of the sample volume before the arrival of the second laser pulse. To overcome this obstacle we would need to gather enough parent ions in the 22-pole ion trap and to use an unfocused or only mildly focused UV beam to pre-excite as much parent molecules as possible.

To ensure rapid cooling of the molecules in the 22-pole ion trap, the ions can be pretrapped in the octopole, where in the collisions with the He gas they loose some of their kinetic energy.

4.2 Experimental setup.

To overcome the problems of low dissociation yields for large biomolecules, a new tandem mass spectrometer was built in the group of Prof. Rizzo [44]. The incorporation of an ion funnel, together with a number of other small technical enhancements significantly improves the sensitivity and signal stability compared to the previous instrumental setup (Figure 10).

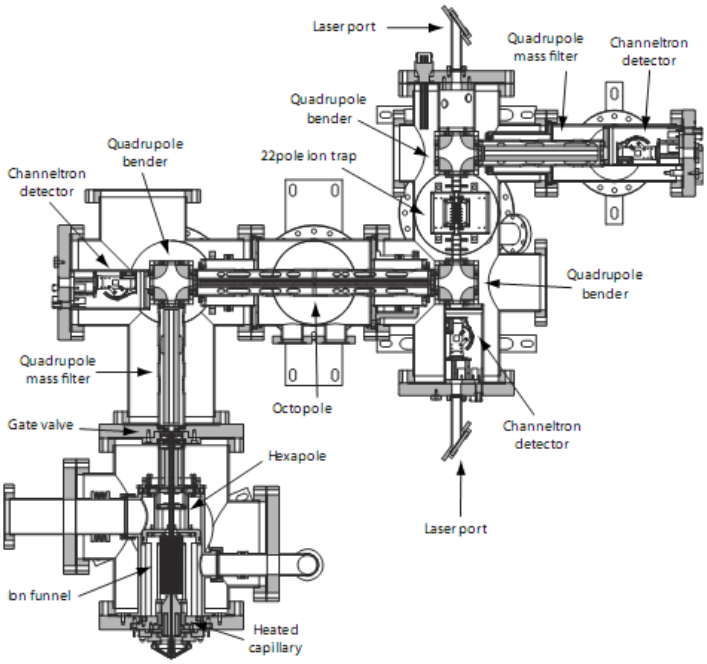

Figure 10. Tandem photofragment mass spectrometer[44].

Biomolecular ions are introduced into the machine by a nanoelectrospray ion source and transferred into vacuum through a metal capillary into an ion funnel composed of a set of rf plates. The ion funnel improves the transmitted ion current by an order of magnitude, as observed by the increase in the number of cold trapped ions from 10^4 to 10^5 (compared to the previous apparatus). Ions leaving the ion funnel can be guided or stored in the hexapole depending on the exit lens potential. The capillary, ion funnel and hexapole are separated from the rest of the machine by a gate valve that highly facilitates cleaning the source.

The next element along the path of the ion package is a quadrupole mass filter, where the ions of a certain mass to charge ratio can be selected. After mass selection, parent ions are deflected into an octopole where they can be guided through or pretrapped before entering the 22-pole ion trap.

The 22-pole ion trap is the central part of the machine. It consists of 22 calibrated stainless steel rods positioned in a circular arrangement. One end of each rod is connected to the copper wall and the other end is loosely supported by a ceramic sleeve in alternating fashion, so that eleven rods are connected to each of the opposite copper walls. The trap assembly is bolted onto a closed-cycle helium cryostat, which enables cooling the trap to approximately 4 K. In order to cool the ions both internally and translationally He gas is injected into the trap through a pulsed valve. When the rf potential is applied to the copper walls of the 22-pole trap, the ions are trapped and cooled down to approximately 10 K. The temperature to which the ions can be cooled depends on their size and can be estimated from hot band intensities in the UV spectrum.

After the parent ions are stored in the 22-pole ion trap for long enough time to cool down, the IR and the UV lasers are shined through and promote the dissociation. Absorption of the UV light can lead to dissociation and the fragments are analyzed with the second quadrupole mass filter. A channel electron multiplier combined with a conversion dynode is used as detector.

5 First experimental results.

The theoretical model introduced in the chapter 3.3 describes the dissociation mechanism of the UV excited peptides in the most simple and general way. To check the validity of this and the other models, it was decided to investigate three different molecules, that Guidi started to study with the IRLAPS technique: Ac-Phe-$(Ala)_5$-$LysH^+$, Ac-$(Ala)_5$-Phe-$LysH^+$ and Ac-Tyr-$(Ala)_5$-$LysH^+$.

Phenylalanine containing peptides showed an approximately one order of magnitude stronger enhancement of the dissociation yield by the IRLAPS technique than Tyr containing peptides. On the other hand, Tyr has the OH group on its aromatic ring, which offers another spectroscopic probe directly connected to the leaving side chain group.

Because the experiments will be carried out on a newly built apparatus, optimization for the best conditions for the ion transport and storing in the machine is necessary. This involves parameters like the voltages, the RF frequencies, the timing delays etc.

The electronic spectrum of Ac-Tyr-$(Ala)_5$-$LysH^+$ was recorded with pretrapping in the octopole for 5 ms (Figure 11). The spectrum revealed well-resolved sharp spectroscopic features that provide an evidence of the effective cooling in the 22-pole ion trap. The infrared spectra of different conformers were recorded using IR-UV double resonance spectroscopy. Though one can clearly distinguish that the spectra are different the noise to signal ratio should be improved, that would be done in the nearest future.

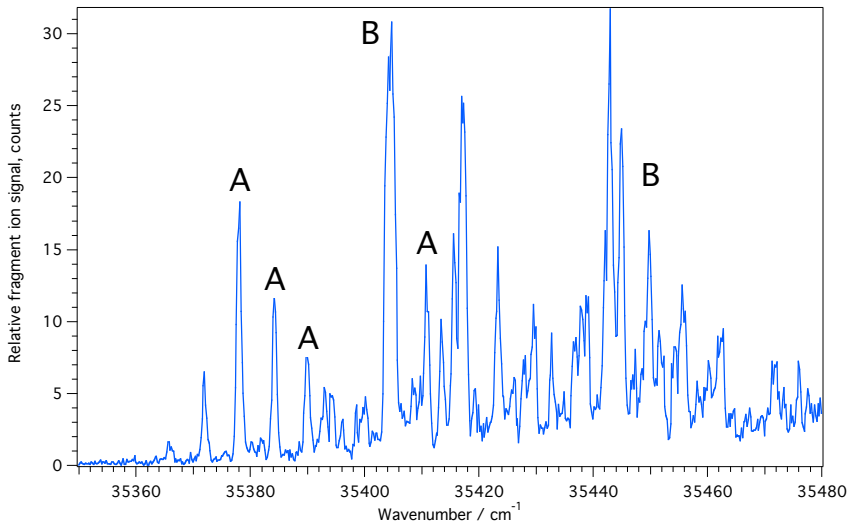

Figure 11. Electronic photofragment spectra of Ac-Tyr-$(Ala)_5$-$LysH^+$. A and B refers to two different conformers.

The UV-IR experiment would be performed as the next step to check if one can fragment the UV pre-excited parent molecules with the infrared laser only.

6 References.

[1] T. R. Rizzo, Y. D. Park, and D. H. Levy, J Chem Phys **85**, 6945-6951 (1986).

[2] T. R. Rizzo, Y. D. Park, L. Peteanu, and D. H. Levy, J Chem Phys **83**, 4819-4820 (1985).

[3] T. R. Rizzo, Y. D. Park, L. A. Peteanu, and D. H. Levy, J Chem Phys **84**, 2534-2541 (1986).

[4] T. R. Rizzo, Y. D. Park, and D. H. Levy, J. Am. Chem. Soc. **107**, 277-278 (1985).

[5] L. C. Snoek, E. G. Robertson, R. T. Kroemer, and J. P. Simons, Chem Phys Lett **321**, 49-56 (2000).

[6] W. Chin, I. Compagnon, J. P. Dognon, C. Canuel, F. Piuzzi, I. Dimicoli, G. von Helden, G. Meijer, and M. Mons, J. Am. Chem. Soc. **127**, 1388-1389 (2005).

[7] W. Chin, J. P. Dognon, F. Piuzzi, B. Tardivel, I. Dimicoli, and M. Mons, J. Am. Chem. Soc. **127**, 707-712 (2005).

[8] W. Chin, F. Piuzzi, J. P. Dognon, L. Dimicoli, B. Tardivel, and M. Mons, J. Am. Chem. Soc. **127**, 11900-11901 (2005).

[9] B. C. Dian, A. Longarte, S. Mercier, D. A. Evans, D. J. Wales, and T. S. Zwier, J Chem Phys **117**, 10688-10702 (2002).

[10] C. Unterberg, A. Gerlach, T. Schrader, and M. Gerhards, J Chem Phys **118**, 8296-8300 (2003).

[11] V. A. Shubert, and T. S. Zwier, J Phys Chem A **111**, 13283-13286 (2007).

[12] J. B. Fenn, M. Mann, C. K. Meng, S. F. Wong, and C. M. Whitehouse, Science **246**, 64-71 (1989).

[13] C. A. Schalley, Int J Mass Spectrom **194**, 11-39 (2000).

[14] P. R. Callis, and J. T. Vivian, Chem Phys Lett **369**, 409-414 (2003).

[15] C. A. Marquezin, L. Y. Hirata, L. Juliano, and A. S. Ito, Biopolymers **71**, 569-576 (2003).

[16] D. Nolting, C. Marian, and R. Weinkauf, Phys Chem Chem Phys **6**, 2633-2640 (2004).

[17] D. Gerlich, Adv. Chem. Phys. **82**, 1-176 (1992).

[18] O. V. Boyarkin, S. R. Mercier, A. Kamariotis, and T. R. Rizzo, J. Am. Chem. Soc. **128**, 2816-2817 (2006).

[19] R. D. F. Settle, and T. R. Rizzo, J Chem Phys **97**, 2823-2825 (1992).

[20] O. V. Boyarkin, and T. R. Rizzo, J Chem Phys **103**, 1985-1988 (1995).

[21] L. I. Yeh, M. Okumura, J. D. Myers, J. M. Price, and Y. T. Lee, J Chem Phys **91**, 7319-7330 (1989).

[22] G. Papadopoulos, unpublished work (2011).

[23] M. Guidi, U. J. Lorenz, G. Papadopoulos, O. V. Boyarkin, and T. R. Rizzo, J Phys Chem A **113**, 797-799 (2009).

[24] M. Guidi, (EPFL, Lausanne, 2010), p. 171 p.

[25] V. Lepere, B. Lucas, M. Barat, J. A. Fayeton, V. J. Picard, C. Jouvet, P. Carcabal, I. Nielsen, C. Dedonder-Lardeux, G. Gregoire, and A. Fujii, The Journal of Chemical Physics **127**, 134313 (2007).

[26] B. Lucas, M. Barat, J. A. Fayeton, M. Perot, C. Jouvet, G. Gregoire, and S. B. Nielsen, The Journal of Chemical Physics **128**, 164302-164307 (2008).

[27] G. Gregoire, C. Jouvet, C. Dedonder, and A. L. Sobolewski, J. Am. Chem. Soc. **129**, 6223-6231 (2007).

[28] G. Gregoire, C. Jouvet, C. Dedonder, and A. L. Sobolewski, Chem Phys **324**, 398-404 (2006).

[29] A. L. Sobolewski, and W. G. Domcke, J Phys Chem A **111**, 11725-11735 (2007).

[30] D. Shemesh, A. L. Sobolewski, and W. Domcke, J. Am. Chem. Soc. **131**, 1374-+ (2009).

[31] L. Joly, R. Antoine, A. R. Allouche, and P. Dugourd, J. Am. Chem. Soc. **130**, 13832-13833 (2008).

[32] A. L. Sobolewski, private communication (2009).

[33] P. D. Schnier, W. D. Price, R. A. Jockusch, and E. R. Williams, J. Am. Chem. Soc. **118**, 7178-7189 (1996).

[34] E. M. Krauss, and S. I. Chan, J. Am. Chem. Soc. **104**, 6953-6961 (1982).

[35] C. Jouvet, private communication (2010).

[36] S. K. Burley, and G. A. Petsko, Adv. Protein Chem. **39**, 125-189 (1988).

[37] D. A. Dougherty, Science **271**, 163-168 (1996).

[38] P. C. Kearney, L. S. Mizoue, R. A. Kumpf, J. E. Forman, A. McCurdy, and D. A. Dougherty, J. Am. Chem. Soc. **115**, 9907-9919 (1993).

[39] J. C. Ma, and D. A. Dougherty, Chemical Reviews **97**, 1303-1324 (1997).

[40] H. Basch, and W. J. Stevens, Theochem-J. Mol. Struct. **338**, 303-315 (1995).

[41] J. P. Gallivan, and D. A. Dougherty, Proc. Natl. Acad. Sci. U. S. A. **96**, 9459-9464 (1999).

[42] J. S. Brodbelt, International Journal of Mass Spectrometry **200**, 57-69 (2000).

[43] M. Heaven, L. Dimauro, and T. A. Miller, Chemical Physics Letters **95**, 347-351 (1983).

[44] A. Svendsen, U. J. Lorenz, O. V. Boyarkin, and T. R. Rizzo, Rev. Sci. Instrum. **81**, -(2010).